Transitional Mixing in a Binary Species Supercritical, Temporal Mixing Layer

Nora Okong'o[+] and Josette Bellan[*]
Jet Propulsion Laboratory
California Institute of Technology
Pasadena, CA 91109-8099
[+]Tel: (818) 393-3149; [*]Tel: (818) 354- 6959, corresponding author; Topic: Mixing

Introduction

The turbulent mixing of fluids at high pressure is a topic of much interest as it is relevant both to natural phenomena and to technical applications. In the realm of technical applications, liquid rocket combustion presents a particular challenge as the operating conditions are supercritical with respect to both fuel and oxidizer, making mandatory the understanding of supercritical fluid behavior for a potentially explosive mixture. In this situation, numerical simulations with validated models can contribute information that would be otherwise impossible to obtain experimentally.

The modeling of supercritical fluid behavior has been primarily addressed in the context of drop modeling. Examples of isolated drop models are those of Umemura and collaborators [29], [30], Curtis and Farrell [3], [4], Jia and Gogos [12], [13], Yang and collaborators [27], [31], Delplanque and Sirignano [6], Daou et al. [5] and Harstad and Bellan [8]. Droplet group effects were modeled by Jiang and Chiang [14], [15], [16] and Harstad and Bellan [9] for monodisperse clusters of drops, and by Harstad and Bellan [11] for polydisperse clusters. Simulations devoted to supercritical shear flows are very scarce (examples being those of Oefelein and Yang [21], [22]) and utilize information obtained from atmospheric pressure turbulence, which introduces uncertainties about their validity. Clearly, a fundamental approach is necessary to unravel the specific aspects of supercritical turbulent shear flows. Such specific aspects have been experimentally observed by Chehroudi et al. [1], [2], and by Mayer and Tamura [18], and include the lack of jet atomization under supercritical condition; instead of drop formation, finger-like structures protruding from the jet are observed.

A contemporary fundamental approach used in fluid mechanics is Direct Numerical Simulation (DNS) whereby all scales of a flow are resolved for Reynolds numbers smaller than those in the fully developed turbulence, but nevertheless reaching the transitional mixing regime. The main artifact of the DNS is to employ a viscosity much larger than that of the real species under consideration so as to enable simulations in a physical domain where the flow is still in the continuum regime. Although this means that the DNS results are not quantitatively correct from the viewpoint of the Reynolds number values, the qualitative behavior of the flow is assumed maintained. Miller et al. [19] have conducted a DNS of a supercritical heptane/nitrogen mixing layer using the validated model of Harstad and Bellan [10] and examined the uncertainties associated with the lack of accurate knowledge of the new transport coefficient, the thermal diffusion factor, which may play an important role at high pressures. However, mixing transition was not achieved in the three dimensional simulation of Miller et al. [19] due to the formation of regions of high density gradient magnitude which acted as material interfaces and damped the emerging turbulent eddies. In fact, Okong'o and Bellan [23] showed that the dissipation correlated well with these regions of high density gradient magnitude, and that the layer evolution was the result of two competing processes: entrainment producing strong density gradients (a stabilizing effect) and mixing reducing the density gradients (a destabilizing effect).

The present study uses the general model of Miller et al. [19] but with modified boundary conditions, a larger forcing amplitude and at higher Reynolds numbers, thereby achieving mixing transition. The details of the simulation are presented in Okong'o and Bellan [24], and therefore only the crucial aspects of the model and simulations will be described below in Section 2. In Section 3, the emphasis of the results is in the specific aspects of the transitional state which reveals visual features that are absent for gaseous layers. Finally, Section 4 is devoted to a summary and conclusions.

Model description

The model is based on the fluctuation-dissipation theory of Keizer [17] whose primary result is the form of the flux matrix which now contains additional terms with respect to the traditional Fick and Fourier contributions. This formulation is moreover consistent with non-equilibrium thermodynamics, and relates from first principles forces and fluxes. The general conservation equations are:

$$\frac{\partial \rho}{\partial t} + \frac{\partial}{\partial x_j}\left[\rho u_j\right] = 0, \tag{1}$$

$$\frac{\partial}{\partial t}\left(\rho u_i\right) + \frac{\partial}{\partial x_j}\left[\rho u_i u_j + p\delta_{ij} - \tau_{ij}\right] = 0, \tag{2}$$

$$\frac{\partial}{\partial t}\left(\rho e_t\right) + \frac{\partial}{\partial x_j}\left[\left(\rho e_t + p\right) u_j - u_i \tau_{ij} + q_{IK,j}\right] = 0, \tag{3}$$

$$\frac{\partial}{\partial t}(\rho Y_h) + \frac{\partial}{\partial x_j}\left[\rho Y_h\, u_j + j_{\alpha j}\right] = 0, \tag{4}$$

where t denotes the time, x is a Cartesian coordinate, subscripts i and j refer to the spatial coordinates, u_i is the velocity, ρ is the density, $e_t = e + u_i u_i/2$ is the total energy (i.e. internal energy, e, plus kinetic energy), p is the thermodynamic pressure, Y_h is the mass fraction of species h (here heptane). Furthermore, τ_{ij} is the Newtonian viscous stress tensor

$$\tau_{ij} = \mu\left[\frac{\partial u_i}{\partial x_j} + \frac{\partial u_j}{\partial x_i} - \frac{2}{3}\frac{\partial u_k}{\partial x_k}\delta_{ij}\right], \tag{5}$$

where δ_{ij} is the Kronecker delta function, and μ is the mixture viscosity which is, in general, a function of the thermodynamic state variables. For a binary mixture, such as the one considered here, we duplicate the form of the fluxes given in [10] by noting that $\mathbf{j}_\alpha = m_\alpha \mathbf{J}_\alpha$ and having α and β take the values h (heptane) and n (nitrogen)

$$q_{IK,j} = -\left[\lambda_{IK}^{'}\frac{\partial T}{\partial x_j} + \alpha_{IK} R_u T\left(\frac{m}{m_n m_h}\right) j_{hj}^{'}\right], \tag{6}$$

$$j_{hj} = -\left[j_{hj}^{'} + \alpha_{BK} Y_n Y_h\, \frac{\rho D}{T}\,\frac{\partial T}{\partial x_j}\right], \tag{7}$$

$$j_{hj}^{'} = \rho D\left[\alpha_D \frac{\partial Y_h}{\partial x_j} + \frac{Y_n Y_h}{R_u T}\left(\frac{m_n m_h}{m}\right)\left(\frac{v_{,h}}{m_h} - \frac{v_{,n}}{m_n}\right)\frac{\partial p}{\partial x_j}\right] \tag{8}$$

where α_{IK} and α_{BK} are the thermal diffusion factors corresponding to the IK and the Bearman-Kirkwood (subscript BK) forms of the heat flux ([26]), respectively; they are the new transport coefficients that are introduced by the Soret (in the molar fluxes) and the Dufour (in the heat flux) terms of the transport matrix, and are characteristic of the particular species pairs under consideration. Properties of these thermal diffusion factors are that $\lim_{p\to 0}\alpha_{IK} \neq \alpha_{KT}$ and $\lim_{p\to 0}\alpha_{BK} = \alpha_{KT}$. According to [10]

$$\alpha_{IK} = \alpha_{BK} + \frac{1}{R_u T}\left(\frac{m_n m_h}{m}\right)\left(\frac{h_{,h}}{m_h} - \frac{h_{,n}}{m_n}\right), \tag{9}$$

and it is thus necessary to specify only one form of the thermal diffusion factors, the two being related by a thermodynamic function. Here the partial molar enthalpy is $h_{,\alpha} = (\partial h/\partial X_\alpha)_{T,p,X_\beta(\beta\neq\alpha)}$, where the molar enthalpy is $h = G - T(\partial G/\partial T)_{p,X}$ with G being the Gibbs energy, and the mole fraction X is related to the mass fraction by $m_\alpha X_\alpha = m Y_\alpha$ where m_α is the molecular weight of pure species α, and the mixture molecular weight is $m = X_n m_n + X_h m_h$. The binary diffusion coefficient is D, the mass diffusion factor is α_D, the thermal conductivity $\lambda_{IK}^{'}$ is defined in [10] from the transport matrix and R_u is the universal gas constant. Furthermore, the molar volume v is related to the mass density by $v = m/\rho$, and the partial molar volume is $v_{,\alpha} = (\partial v/\partial X_\alpha)_{T,p,X_\beta(\beta\neq\alpha)}$. It can be shown that $\lambda_{IK}^{'}$ does not correspond to the kinetic theory (subscript KT) definition of the thermal conductivity in that $\lim_{p\to 0}\lambda_{IK}^{'} \neq \lambda_{KT}$ but it is related to the thermal conductivity, λ, through

$$\lambda_{IK}^{'} = \lambda + X_n X_h\, \alpha_{IK}\, \alpha_{BK} R_u \rho D/m. \tag{10}$$

where $\lim_{p\to 0}\lambda = \lambda_{KT}$ as discussed in [10]. The mass diffusion factor α_D is also a thermodynamic function which is calculated from the fugacity coefficients, φ_α (which are related to the Gibbs energy), as follows:

$$\alpha_D = 1 + X_\alpha \frac{\partial \ln(\varphi_\alpha)}{\partial X_\alpha}, \tag{11}$$

Note that α_D is independent of which species is chosen in the evaluation.

The details of the adopted equation of state are presented in Miller et al. [19] and will not be duplicated herein. It suffices to state that a Peng - Robinson equation of state is utilized with mixing rules proposed by Harstad et al. [7], and that this choice is both computationally efficient and reasonably accurate since the pure species reference states were found to be accurate to better than 1% relative error through comparisons with the accurate state equations of [7] over the range of variables used in this study.

The configuration used is that of a three-dimensional temporal mixing layer shown in Fig. 1, whose lower stream is heptane and upper stream is nitrogen. The boundary conditions employed are periodic in the streamwise and spanwise directions and outflow conditions based on a characteristic wave approach for real gases as described in Okong'o et al. [25]. The employed disturbance, and the characteristics of the domain size are discussed by Okong'o and Bellan [24] and will not be repeated here.

Particular care was devoted to represent the transport coefficients in a self consistent manner, based on contour plots of the Schmidt, Sc, and Prandtl, Pr, numbers using accurate transport properties. Accordingly, the following simplified expressions were used to represent the transport coefficients

$$\mu = \mu_R\left(\frac{T}{(T_1+T_2)/2}\right)^{0.7}; \qquad T \text{ in Kelvins}, \tag{12}$$

$$Sc = \frac{\mu}{\rho\alpha_D D} = 1.5 - Y_h, \quad \mathrm{Pr} = \frac{\mu C_p/m}{\lambda} = \frac{Sc}{2\exp(-3Y_h/2)}, \tag{13}$$

where μ_R is a reference viscosity and the reference temperatures T_1 and T_2 correspond to the free stream temperatures for mixing layer simulations. These relations give qualitatively correct trends in that Sc is respectively greater than or less than unity for the proper mass fractions; however, the maximum value is 1.5 rather than 2, as observed in the contour plots. Eqs. 12 - 13 hold in the

following range of thermodynamic state space: $500K \leq T \leq 1100K$, $6kg/m^3 \leq \rho \leq 286kg/m^3$, and $0 \leq Y_h \leq 1$.

The value of the reference viscosity is determined by the specified value of the initial Reynolds number

$$\mathrm{Re}_0 = \frac{0.5(\rho_1 + \rho_2)\Delta U_0 \delta_{\omega,0}}{\mu_R} \tag{14}$$

chosen so as to enable the resolution of all relevant dynamic length scales. The freestream density (ρ_1 or ρ_2) is calculated for each pure species at its freestream temperature (T_1 or T_2) and at the initial uniform pressure (p_0). The vorticity thickness is defined as $\delta_\omega(t) = \Delta U_0 / \left(\partial U/\partial x_2\right)_{max}$ where U is the mean (or $x_1 - x_3$ planar average) flow in the streamwise direction, and $\Delta U_0 = U_1 - U_2$ is the velocity difference across the layer. Miller et al. [19] explain the choice of the velocities of the two streams, the intent being to keep the vortices stationary in the computational domain. Whereas the success in this endeavor was only partial, it proved that the choice of

$$U_1 = 2M_c a_{s_1}\left[1 + \left(\frac{a_{s_1}}{a_{s_2}}\right)\sqrt{\frac{\rho_1 Z_1}{\rho_2 Z_2}}\right]^{-1}, \quad U_2 = -\sqrt{\frac{\rho_1 Z_1}{\rho_2 Z_2}}U_1, \tag{15}$$

for a real fluid was reasonable, where M_c is a Mach number and $Z = p/(\rho T R_u/m)$ is the compression factor. The specification of M_c therefore determines ΔU_0, and thus ultimately $\delta_{\omega,0} \equiv \delta_\omega(0)$. The mean streamwise velocity is smoothed near the centerline using an error function profile, as are the mean temperature and mass fraction.

The adopted value of the thermal diffusion factor is $\alpha_{IK} = 0.1$, determined by Harstad and Bellan [10] first from a model calibration through comparisons with part of the data from the microgravity experiments of Nomura et al. [20], and further validated in the same study by comparison with the remaining part of Nomura et al.'s [20] data.

Results

The results focus on the characteristics of the transitional state and its peculiarities compared to purely gaseous mixing layers. Global features of the mixing layer are assessed for two values of Re_0. These global features as well as detailed vorticity contour plots show that transition has been attained. Various characteristics of the fluid are documented at the transitional state, in particular departures from mixing ideality and perfect gas behavior. Moreover, scrutiny of the dissipation shows that it is mostly of viscous nature, although the non-ideality term may contribute considerably to backscatter.

Summary and conclusions

A model of a supercritical shear layer has been utilized with appropriate boundary conditions to study the transition of a supercritical shear layer to a turbulent state. The achievement of turbulence has been ascertained both from global features of the layer and from detailed contour plots at the transitional state. The state of the fluid at the transitional state has been determined, showing strong departures from ideality and perfect gas behavior. Specific optically related features of the layer that are due to the density stratification have been documented. Various aspects of the dissipation have been explored and it has been shown that non-ideality may play an important role in the correct modeling of backscatter.

Acknowledgments

This research was conducted at the Jet Propulsion Laboratory (JPL), California Institute of Technology. Joint sponsorship was provided by the Air Force Office of Scientific Research with Dr. Julian Tishkoff serving as contract monitor and by the Army Research Office with Dr. David Mann as technical contract monitor, through interagency agreements with the National Space and Aeronautics Administration (NASA). Computational resources were provided by the supercomputing facility at JPL. The authors wish to thank Dr. Mark Carpenter of NASA Langley Research Center and Dr. Kenneth Harstad of JPL for helpful discussions.

References

[1] Chehroudi, B., Talley, D. and Coy, E., Initial growth rate and visual characteristics of a round jet into a sub- to supercritical environment of relevance to rocket, gas Turbine, and Diesel engines, AIAA 99-0206, 37th Aerospace Sciences Meeting, Reno, NV, 1999

[2] Chehroudi, B., Talley, D. and Coy, E., Fractal geometry and growth rate changes of cryogenic jets near the critical point, AIAA 99-2489, 35th AIAA/ASME/SAE/ASEE Joint Propulsion Conference, Los Angeles, CA, 1999

[3] Curtis and Farrell, P. V., Droplet vaporization in a supercritical microgravity environment, *Acta Astronautica*, 17(11/12), 1189-1193, 1988

[4] Curtis and Farrell, P. V., A numerical study of high-pressure droplet vaporization, *Combust. Flame*, 90, 85-102, 1992

[5] Daou, J., Haldenwang, P. and Nicoli, C., Supercritical burning of liquid oxygen (LOX) droplet with detailed chemistry, *Combust. Flame*, 101, 153-169, 1995

[6] Delplanque, J-P. and Sirignano, W. A., Numerical study of the transient vaporization of an oxygen droplet at sub- and super-critical conditions, *Int. J. Heat Mass Transfer*, 36(2), 303-314, 1993

[7] Harstad, K. G. , Miller, R. S., and Bellan, J., Efficient high pressure state equations *A. I. Ch. E.* 43(6), 1605-1610, 1997

[10] Harstad, K. and Bellan, J., An all-pressure fluid drop model applied to a binary mixture: heptane in nitrogen, *Int. J. of Multiphase Flow*, 26(10), 1675-1706, 2000

[11] Harstad, K. and Bellan, J., The d^2 variation for isolated LOX drops and polydisperse clusters in hydrogen at high temperature and pressures, accepted for publication, *Comb. Flame*, 2000

[12] Jia, H. and Gogos, G., Investigation of liquid droplet evaporation in subcritical and supercritical gaseous environments, *Journal of Thermophysics and Heat Transfer*, 6(4), 738-745, 1992

[13] Jia, H. and Gogos, G., High pressure droplet vaporization; effects of liquid-phase solubility, *Int. J. Heat Mass Transfer*, 36(18), 4419-4431, 1993

[14] Jiang, T. L. and Chiang, W-T., Effects of multiple droplet interaction on droplet vaporization in subcritical and supercritical pressure environments, *Comb. Flame*, 97, 17-34, 1994

[15] Jiang, T. L. and Chiang, W-T., Vaporization of a dense spherical cloud of droplets at subcritical and supercritical conditions, *Combust. Flame*, 97, 355-362, 1994

[16] Jiang, T. L. and Chiang, W-T., Transient heating and vaporization of a cool dense cloud of droplets in hot supercritical surroundings, *Int. J. Heat Mass Transfer*, 39(5), 1023-1031, 1996

[17] Keizer, J., *Statistical Thermodynamics of Nonequilibrium Processes*, Springler-Verlag, New York, 1987

[18] Mayer, W. and Tamura, H., Propellant injection in a liquid oxygen/gaseous hydrogen rocket engine, *Journal of Propulsion and Power*, 12(6), 1137-1147, 1996

[19] Miller, R. S., Harstad, K. and J. Bellan, J., Direct numerical simulations of supercritical fluid mixing layers applied to heptane nitrogen, submitted for publication to *J. Fluid Mech.*, 1999

[20] Nomura, H., Ujiie, Y., Rath, H. J., Sato, J. and Kono, M., Experimental study on high pressure droplet evaporation using microgravity conditions, *Proc. of the Comb. Institute*, 26, 1267-1273, 1996

[21] Oefelein, J. C. and Yang, V., Analysis of transcritical spray phenomena in turbulent mixing layers, AIAA 96-0085 34^{th} Aerospace Sciences Meeting, Reno, NV., 1996

[22] Oefelein, J. C. and Yang, V., Analysis of hydrogen-oxygen mixing and combustion processes at high-pressures, AIAA 97-0798 35^{th} Aerospace Sciences Meeting, Reno, NV., 1997

[23] Okong'o, N. and Bellan, J., Entropy production of emerging turbulent scales in a temporal supercritical n-heptane/nitrogen three-dimensional mixing layer, *Proc. of the Comb. Institute*, 28, 2000, in press

[24] Okong'o, N. and Bellan, J., Direct numerical simulation of a transitional supercritical mixing layer: heptane and nitrogen, submitted to *J. Fluid Mech.*, 2000

[25] Okong'o, N., Bellan, J. and Harstad, K., Consistent boundary conditions for multicomponent real gas mixtures based on characteristic waves, submitted to the *J. Comp. Phys*, 2000

[26] Sarman, S. and Evans, D. J., Heat flux and mass diffusion in binary Lennard-Jones mixtures, *Phys. Rev.* A45(4), 2370-2379, 1992

[27] Shuen, J-S., Yang, V. and Hsiao, G. C., Combustion of liquid-fuel droplets in supercritical conditions, *Combust. Flame*, 89, 299-319, 1992

[28] Shuen, J-S. and Yang, V., Combustion of liquid-fuel droplets in supercritical conditions, AIAA 91-0078, 29th Aerospace Sciences Meeting, January 7-10, Reno, NV, 1991

[29] Umemura, A., Supercritical liquid fuel combustion, *Proc. of the Comb. Institute*, 21, 463-471, 1986

[30] Umemura, A. and Shimada, Y., Characteristics of supercritical droplet gasification, *Proc. of the Comb. Institute*, 26, 1621-1628, 1996

[31] Yang, V., Lin, N. and Shuen, J-S., Vaporization of liquid oxygen (LOX) droplets in supercritical hydrogen environments, *Combust. Sci. and Tech.*, 97, 247-270, 1994

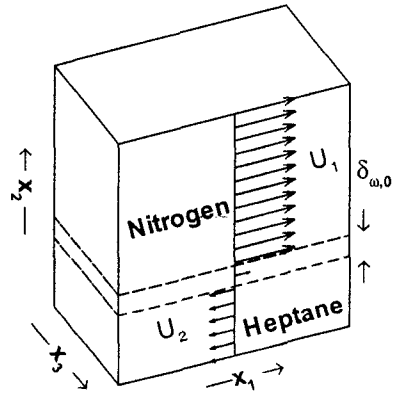

Figure 1: Shear layer configuration